

FLUX DENSITY AND BREAKTHROUGH TIMES FOR WATER AND TRACER IN A SPATIALLY VARIABLE, COMPACTED CLAY SOIL

ANDREW S. ROGOWSKI

USDA-ARS, Northeast Watershed Research Center, University Park, PA 16802, U.S.A.

(Received September 5, 1987; revised and accepted March 25, 1988)

ABSTRACT

Rogowski, A.S., 1988. Flux density and breakthrough times for water and tracer in a spatially variable, compacted clay soil. In: P.F. Germann (Editor), *Rapid and Far-reaching Hydrological Processes in the Vadose Zone. J. Contam. Hydrol.*, 3: 327–348.

Flux density values, computed from observed infiltration and outflow measurements at 184 locations in a 0.3-m-thick, 9 m × 23 m layer of compacted clay subsoil, are compared to effective flux density values that are based on breakthrough time distributions for water and Br⁻ tracer over the same area. Results suggest that both water and tracer move at similar rates, but considerably faster than expected, on the basis of flux density alone, and that only a small fraction of the total pore space is involved in active transport. The ramifications of these findings are explored against the background of effective porosity, degree of compaction, and observed changes in bulk density with time.

INTRODUCTION

The deterioration of groundwater quality is a serious problem on a national as well as regional scale. Industrial and agricultural point and nonpoint sources contribute to this degradation, as do waste-disposal sites. Waste-disposal sites need improved evaluation and testing during and after construction, while agricultural areas require a more accurate assessment of pollution potential on a field scale prior to applications of manure, fertilizer, pesticides, and herbicides. In most cases, pertinent parameters and relevant flow pathways need to be identified and improved field sampling techniques developed. One such promising field parameter is the distribution in time of water flux over an area.

Water flux, expressed as flux density (q) and also known as Darcy velocity, specific flux, or specific discharge, has the dimensions of length per unit time. Flux may be defined as the volume of water (Q) moving through a unit cross-sectional area (A) of soil per unit of time:

$$q = Q/A \quad (1a)$$

It can also be written in the simple form of Darcy's Law as:

$$q = KJ \quad (1b)$$

where J is the dimensionless gradient arising from differences in head and K is the coefficient of permeability (hydraulic conductivity). If the cross-sectional area is at the soil surface, q is an infiltration rate; if at the water table, q is recharge; if somewhere between the surface and the water table, q is simply a flux density at a given depth.

Under saturated isothermal conditions in an isotropic nonswelling porous medium, K is assumed constant and laboratory values measured on cores are expected to describe completely the permeability distribution in the field. This, however, is not always the case (Daniel, 1984), even under carefully controlled experimental conditions. The disparity between laboratory- and field-determined values of hydraulic conductivity has raised questions regarding the integrity of clay liners in containment facilities and pollution potential of agricultural and industrial sites. The problem is not unique to engineered structures; it is also found in geology and natural field soils.

Moreover, clay liners used in many containment facilities and compacted to engineering specifications of better than 90% Standard Proctor even when ponded are seldom saturated. Darcy's Law has been extended to unsaturated conditions, where K depends on the degree of water saturation and temperature, while gradient J is taken as a function of total potential (Nielsen et al., 1986). In compacted clay liners, which are unsaturated in the strict sense of the word, little change in water content with time is expected because of intentionally low values of matrix hydraulic conductivity, entrapped air, and discontinuous pores. If, however, a site as a whole exhibits flux that is higher than would be expected, existence of areas with preferential-flow pathways and presence of short-circuiting flows may be suspected.

Short circuiting, which occurs in a few relatively larger cracks, fissures, or pores, may essentially bypass the rest of the soil. If the short-circuiting is connected to the surface, it may be quite sensitive to changes of head in ponded water. Even if not connected to the surface the condition for seepage into such cavities (Philip, 1987) is that the pressure at some point of the cavity wall can reach atmospheric (or equal the internal pressure within the cavity). A similar principle applies to solid inclusions like stones and rock fragments. Consequently, areas with rapid water or tracer breakthrough and high flux-density values may often be indicative of preferential-flow path locations. To understand how preferential-flow pathways operate, it is important to identify such locations and to study their behavior and spatial response in time.

Thus, the primary objective of this study reported here was to examine the behavior of high flux-density zones, observed within a compacted experimental clay liner. This was accomplished by studying the fate of introduced tracer, by monitoring inflow and outflow, by computing breakthrough time, and by identifying flow pathways in a compacted clay layer in a specially constructed testing facility.

METHODS

Testing facility

The testing facility (Fig. 1) consisted of a bridge-like 9×23 m reinforced concrete platform (Rogowski et al., 1985). A grid (0.9×0.9 m) of leachate-collection drains under compacted clay was complemented by a similar grid of 30-cm diameter infiltration rings. Twenty-cm-high infiltration rings were driven into the soil at the surface to the depth of 8 cm. Figure 2 shows respective grids for sampling bulk density (a), inflow and outflow (b), extent of swelling and evaporation (c), and tracer distribution (d). Their origin (0,A) is the southwest corner of the platform.

Imbedded in the floor of the platform and positioned horizontally across the facility were the lower access tubes (Fig. 1) for the measurement of bulk density with the Troxler¹ dual gamma probe. Positioned on the clay surface, 30 cm above the lower access tubes, were the upper access tubes. The attenuation measurements were made horizontally at 240 locations with a gamma source (Cs^{137}) in the lower tube and with a detector in the upper tube. The degree of attenuation was used to compute bulk density in a conical volume of soil between the source and the detector. Measurements were made continuously and sequentially. It took approximately three days to complete one set of 240 readings before the next set was begun. In this way 13 sets of readings were taken prior to ponding, 64 sets following ponding, and 2 sets after draining the ponded water — about 19,000 observations in all.

Since no substantial swelling was observed (Rogowski, 1985), changes in soil bulk density with time were expected to reflect changes in soil water content as water moved into and through the clay matrix. For highly compacted and

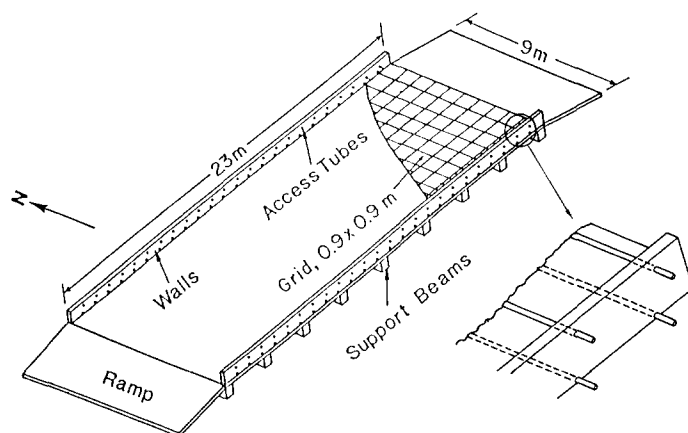


Fig. 1. Clay liner testing facility.

¹The mention of trade names in this publication does not constitute an endorsement of the product by the United States Department of Agriculture over other products not mentioned.

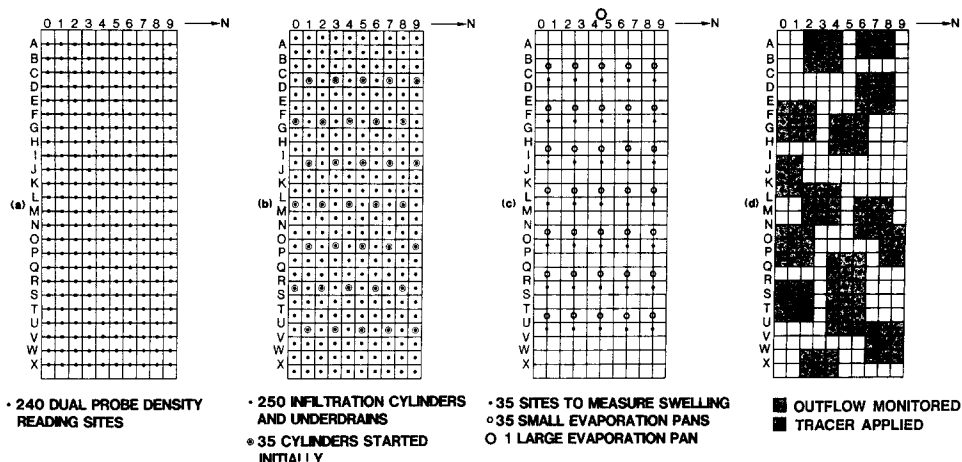


Fig. 2. Experimental 0.91 × 0.91 m grids used in measuring (a) bulk density, (b) infiltration and outflow, (c) swelling and evaporation, (d) tracer breakthrough.

ponded soils, when steady-state conditions are attained, changes in soil water content should cease, and measured distribution of flux should reflect primarily the water flow through more rapidly conducting cracks, channels, and other preferential-flow pathways.

The soil used was a B-horizon of a Typic Hapludult cherty silt loam from central Pennsylvania. It was compacted wet at optimum to greater than 90% Standard Proctor with a sheepsfoot roller (Rogowski and Richie, 1984). At this moisture content, matrix potential for compacted soil was approximately 100 kPa. The soil was classified as a CL type, having a permeability of 0.1 to $0.2 \times 10^{-9} \text{ ms}^{-1}$, as determined in a laboratory with a falling head permeameter at 90% maximum density and a gradient of about 20. Mineralogically it is a mixture of illite and kaolinite with minor amounts of montmorillonite. Figure 3 shows spatial distribution of sand, silt, and clay in the compacted material.

Instrumentation

An experimental clay liner was constructed in three lifts, using heavy equipment and incorporating water to bring the soil to a uniform water content and density. Spatial distribution of bulk density and water content are shown in Fig. 4a and b, respectively. In addition to bulk density, infiltration rate was measured in 184 infiltration rings at the surface, and outflow rate was monitored in 184 vertical drains situated below the clay and directly under the rings. In addition, there were 35 sites to evaluate swelling and 1 class A evaporation pan and 35 small evaporation pans (same size as infiltration rings) to measure evaporation. After the experimental clay liner was constructed and instrumented, it was ponded, and the water level was maintained constant with

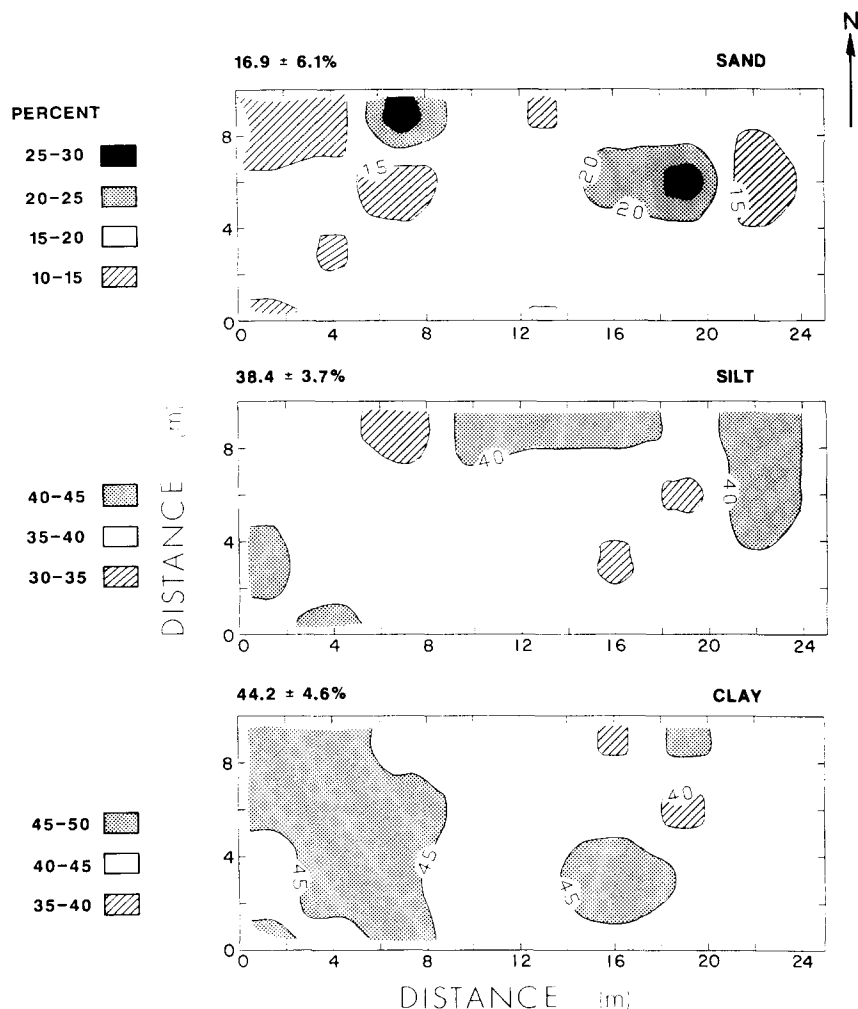


Fig. 3. Distribution of sand, silt, and clay in compacted, spatially variable clay liner.

an automatic constant head tank. Times of the first arrival of water in outflow drains were recorded and initially only 35 infiltration sites were monitored. Subsequently all infiltration rings and small evaporation pans were equipped with 1-L Mariotte constant head bottles, set to the same level as the ponded water outside. Individual leachate drains were routed to the outside of the platform, and leachate was collected and composited weekly. Water level changes in small evaporation pans were used to correct infiltration data for the amounts of water that evaporated between readings. Collection of leachate began immediately after ponding but it was about 3 months before all infiltration rings could be read at the same time (Rogowski, 1985). Results reported here are based on 36 sets of readings that were composited weekly beginning

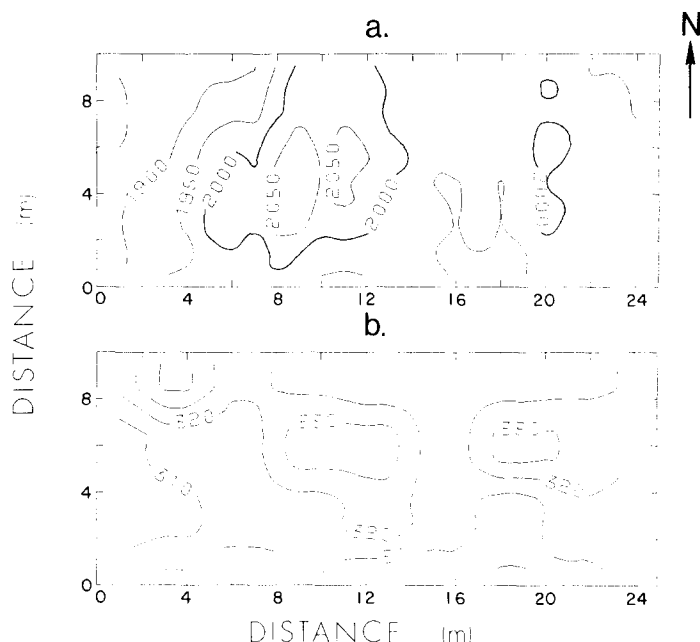


Fig. 4. Contours of average density (in kg m^{-3}) (a) and water content (in kg m^{-3}) (b) on the experimental clay liner before ponding.

in June 1985 for each of the inner 184 rings and drains (about 6600 values). The last set of readings was composited over 2 months because of small inflow and outflow amounts. The 66 outer rings and drains next to the edge and sides of the platform served as a buffer and are not included in calculations.

Tracer studies

Tracer studies were initiated at the conclusion of the main experiment. To prepare the tracer, 1 g molecular weight of KBr (0.119 kg) was dissolved in 1L of water to give 1M solution of Br^- (0.079 kg L^{-1}). Either 50 or 100 mL of this solution were diluted with ponded water to 2000 mL and added to 15 rings (Fig. 2d) in one, two, or three 2000 mL increments, depending on the observed flux rates and projected travel time. When tracer solution was applied to a ring, "time zero" samples of leachate from the underlying drain and eight surrounding drains were taken. Sampling of leachate was continued at suitable intervals that depended on the volume of accumulated outflow. Leachate samples were analyzed for Br^- content using a ion-specific bromide electrode.

Computations

Distribution of effective porosity can be estimated when distribution of breakthrough time (T_b) at some depth (L), taken as the first arrival of water or tracer, is available. Effective porosity (P_e) is a ratio between average effective

cross-sectional flow area (A_e) and unit cross-sectional flow area (A), while effective flux density (q_e), also known as average pore water velocity (Kirkham and Powers, 1972), can be written:

$$q_e \geq L/T_b \quad (2)$$

Since $q = Q/A$ and, analogously, $q_e = Q/A_e$:

$$A_e \leq \frac{QT_b}{L} \quad (3)$$

and

$$P_e = A_e/A = q/q_e \quad (4)$$

RESULTS AND DISCUSSION

Time to equilibrium

Figure 5 shows the distribution of average inflow and outflow during a one-year study period for the experimental clay liner as a whole. Initial decline in inflow rate at ponding was followed by a rise and subsequent decline in both inflow and outflow. The rise and decline at 8–9 months coincides with the time when approximately one pore volume of water on the average has passed through the clay. Such fluctuations in observed flow rate should be viewed in proper perspective, since they represent a net difference of only $\sim 0.3 \text{ cm day}^{-1}$ in water level elevation and appear to have several possible explanations (Rogowski, 1986a).

The data suggest that there was a slow negative pressure buildup under the clay, because initially the drain lines were not vented. Intermittent buildup and drainage of water in each of the 184 outlet tubes could selectively impose a small tension ($< 60 \text{ cm}$ of water) on the underside of the clay. As more and

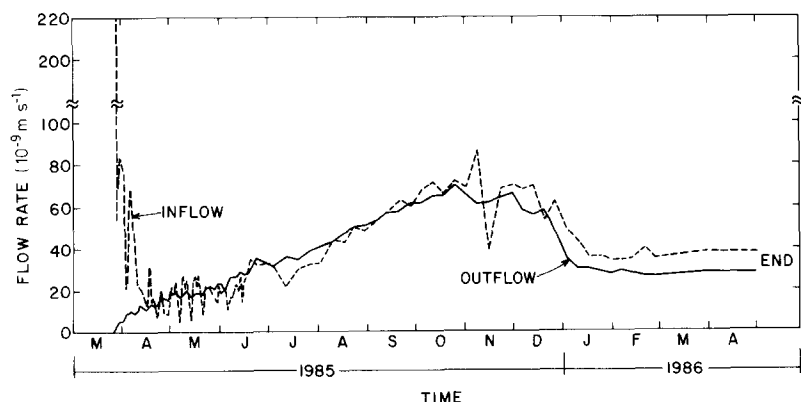


Fig. 5. Average inflow (dashed) and outflow (solid) rate during a one-year study period for the experimental clay liner.

more drains became active, the effect increased, becoming particularly noticeable for fast-flowing drains associated with macropore flow. Soon after the drains were vented in December 1985, flow rate declined and an apparent equilibrium was established. These results may be of considerable practical significance, since venting of the underside of in place clay liners could lower their effective permeability.

However, since the decline in flux rate had already begun for some drains before the drains were vented, another possible explanation is that infiltration and outflow rates were affected by temperature, ionic composition of water, and changes in amounts of entrapped air. Temperature effects are primarily due to differences in viscosity. Temperatures at the site were often in excess of 25°C during summer and early fall but were maintained at 5°C in the winter. The difference could account for more than 50% increase in viscosity, reducing the corresponding flow rate by as much as 1/3.

The ambient pressure developed within individual pores and the amount of entrapped air that dissolves in pore water are also highly dependent on temperature. Since cold water can hold more air than warm, decline in temperature can lead to shrinkage of entrapped air vacuoles and localized increases in flow. However, if cold water enters the warmer clay matrix, air may go out of solution, leading to air blockage in some pores. It is felt that the decline of flow rate through clay in January was in part associated with decreased viscosity, but it is doubtful if and to what extent temperature affected entrapped air within the clay matrix.

Finally, differences in the ionic composition of ponded water and leachate could alter the flow rate through clay. In particular, differences in Na^+ and Ca^{2+} concentrations could lead to localized dispersion and aggregation, either blocking or opening individual pores. During the construction of the experimental clay liner, a layer of burlap, followed by a thin layer of sand (0.6 cm), was placed under the compacted clay. Prior to the venting of drains, anaerobic denitrification with abundant Fe^{3+} , serving as an energy source for microorganisms that utilize the burlap substrate, could have taken place. Soluble Fe^{++} could then be preferentially leached out, oxidizing, precipitating, and clogging some pores when it came in contact with air. Precipitated iron, calcium, and manganese were the primary deposits in outflow tubes and catchment containers. The amount varied, being highest for the slow flowing drains. In final analysis it is felt that a combination of all these factors taken together may be responsible for a rise, subsequent decline, and eventual equilibration of observed average inflow and outflow rates.

Once the steady state was established, the net difference between inflow and outflow rate in Fig. 5 was on the order of $10 \times 10^{-9} \text{ m s}^{-1}$, a change in water level equal to $0.086 \text{ cm day}^{-1}$, well within experimental error of the monitoring equipment. Results for a compacted, 30-cm-thick clay liner showed that it took almost a year to attain steady state under our experimental conditions. For thicker layers the time to equilibrium could be comparatively longer.

Figure 6 shows the distribution of average bulk density for the same time

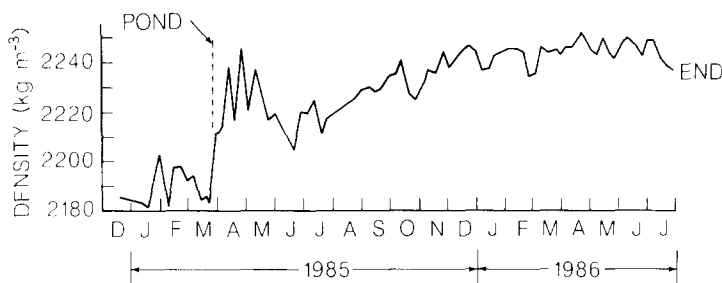


Fig. 6. Average bulk density measured with a dual gamma probe during a one-year study period on an experimental clay liner.

period as the previously discussed inflow and outflow distributions. Bulk density increased through March of 1986, becoming more or less constant after that time. In addition, average density values observed before ponding (POND) are also given. The increasing bulk density after ponding, like inflow and outflow, reached the steady state in about 11–12 months. Variations shown in April and May 1985 were due to a temporary probe malfunction.

Changes in time of flow and bulk density

Values of inflow and outflow in Fig. 5 and bulk density in Fig. 6 are space averages in time taken over 184 drains and rings or 240 access tube locations. These should be contrasted with data (Fig. 7) that show changes in inflow, outflow, and density at a specific point in time. Figure 7 illustrates how flow

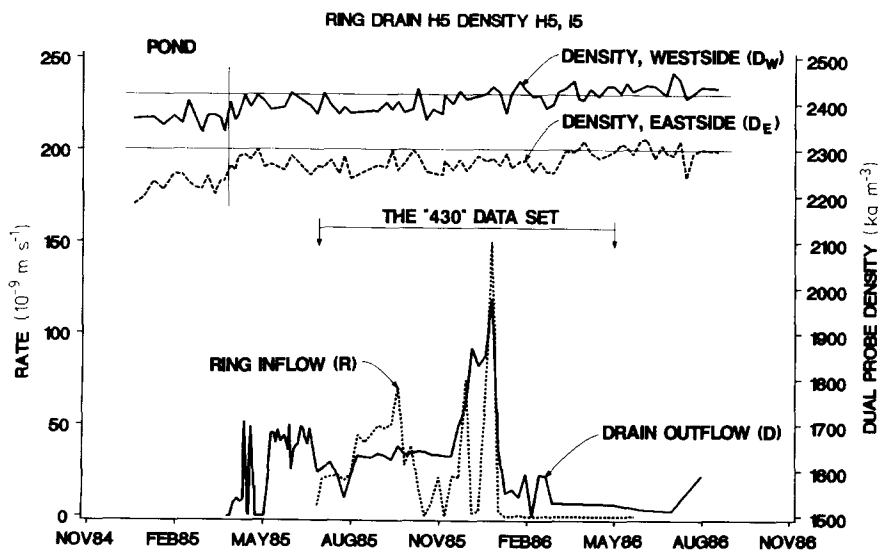


Fig. 7. Distribution in time of ring inflow (R) and drain outflow (D) at the site H5 and of bulk density at adjoining sites to the west (D_W) and east (D_E) of the ring/drain site (H5, I5).

and bulk density did vary at a location where rapid breakthrough of water and tracer has been observed. Some possible reasons for these fluctuations were discussed earlier. Since this location appeared to be in the zone of high flux density (Rogowski and Simmons, 1988), observed behavior could also reflect preferential flow pathway response at a point. Figure 7 shows typical flow (lower) and bulk density (upper) patterns recorded during the study. The ring (R) inflow and drain (D) outflow rates are given by the left-hand scale, while bulk density values, measured east (D_E) and west (D_W) of the respective ring and drain locations, are shown on the right-hand scale. Thin horizontal lines through bulk density values are included to highlight any trends in the data, while a thin vertical line indicates the time of ponding. The values are for the H5 and I5 locations of bulk density (Fig. 2a) and H5 location of ring inflow and drain outflow (Fig. 2b). Arrows in Fig. 7 denote a time span associated with the "430" data set. This particular set consists of flow volumes (taken as inflow or outflow), summed up over an 11-month period and divided by the total elapsed time.

Visual comparisons of bulk density distributions with thin lines show little change in bulk density with time. For this location, as well as for some others not shown here, there is usually a small increase following ponding and a very gradual and also small increase with time. Yet results in Fig. 6 show that, on the average, density increased by about 50 kg m^{-3} before becoming constant at about 11–12 months. Such increases may represent the extent of water movement into the clay where about half of it occurs immediately after ponding and half is spread over the following nine months. This could mean that the initially observed change in bulk density was due to relatively rapid filling of preferential flow pathways and wetting of soil surface, while additional water diffused more slowly into the clay matrix. Speaking quantitatively, observed changes amounted to a modest increase in soil density, but because of high compaction and water content they constituted as much as 15–20% change in available porosity.

Comparison of water and tracer breakthrough

Tracer tests with Br^- were carried out towards the end of the study, while water breakthrough times, given as first arrival of water at the respective drains, were recorded immediately following ponding. Bromine was chosen as a tracer because of its conservative behavior and low background concentrations. Although anion exclusion and Br^- reactions with positively charged portions of the clay matrix may affect tracer movement, short-circuiting flows through the macropores should be relatively free of these considerations, either because the flow is more rapid, or because the size of transporting pores is much larger than the rest of pores in the clay matrix.

Tracer breakthrough, given as the first arrival of tracer at the principal drain or one of the surrounding drains, originated from a centrally positioned, 600-cm^2 infiltration ring. Water breakthrough, however, was a result of

ponding the entire facility, and outflow from a 8000-cm² area surrounding each drain. In either case, the clay liner was not fully saturated. Initial water-content distribution (Fig. 4b) corresponded to a 100-kPa tension, while water contents after the water was drained were no more than 3% higher throughout. Under these conditions, observed breakthrough times would most likely be a result of short-circuiting flow through the macropores.

Figure 8 shows histograms of water and tracer breakthrough data, and Fig. 9 gives raw semivariogram values (points) and corresponding fitted models. The histogram in Fig. 8a gives the distribution of breakthrough times for water, which is represented by substantial frequencies in all classes. However, breakthrough times for tracer (Fig. 8b) are heavily skewed and primarily confined to 1 frequency class. All semivariogram points are based on more than 79 pairs comparison, while the range of experimental models, given as 1.8 and 5.6 m for tracer and water, respectively, is well within the zone of influence for each situation (Journel and Huijbregts, 1978). Semivariance structure suggests good continuity and low nugget effect for water breakthrough data and essen-

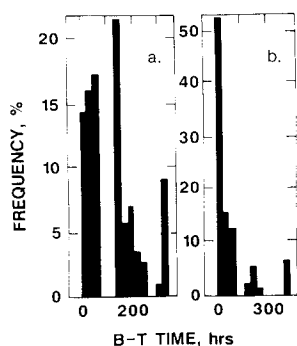


Fig. 8. Frequency histograms of breakthrough times (B-T time) for water (a) and Br^- tracer (b).

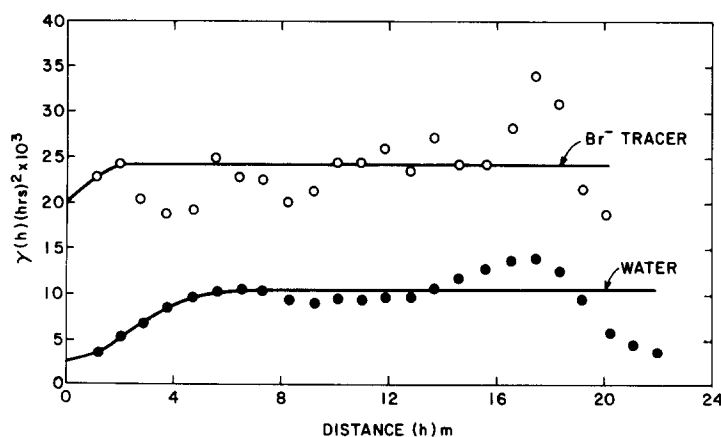


Fig. 9. Raw semivariograms and fitted models for water and tracer breakthrough times.

tially no structure and almost a pure nugget effect for Br^- tracer. The difference between the two may be due to fewer values, smaller "support" (600 versus 8000 cm^2), and irregular nature of support for tracer data (Fig. 2d). The discontinuity of both variograms at the origin (nugget effect) may have been caused by measurement errors and variability on a scale smaller than the scale of measurement (Cressie, 1987). Tracer breakthrough distribution represents samples of continuum, while water breakthrough distribution following ponding represents the whole continuum. Thus, tracer data in general appear independent of one another beyond a 1.8-m range, while water breakthrough values have a much larger (~ 6 m) continuity range that essentially spans the width of the facility.

The results suggest that spatial distribution of outflow (and also perhaps of inflow) may consist of a bimodal field, one part of which is composed of continuous, highly correlated values of matrix flux density. The other is essentially a random distribution of preferential-flow pathway clusters superimposed on the clay matrix. The notion is similar to the concepts of flow in "structured soils" discussed by Nielsen et al. (1986).

In Fig. 10, results for tracer and water breakthrough times are presented as

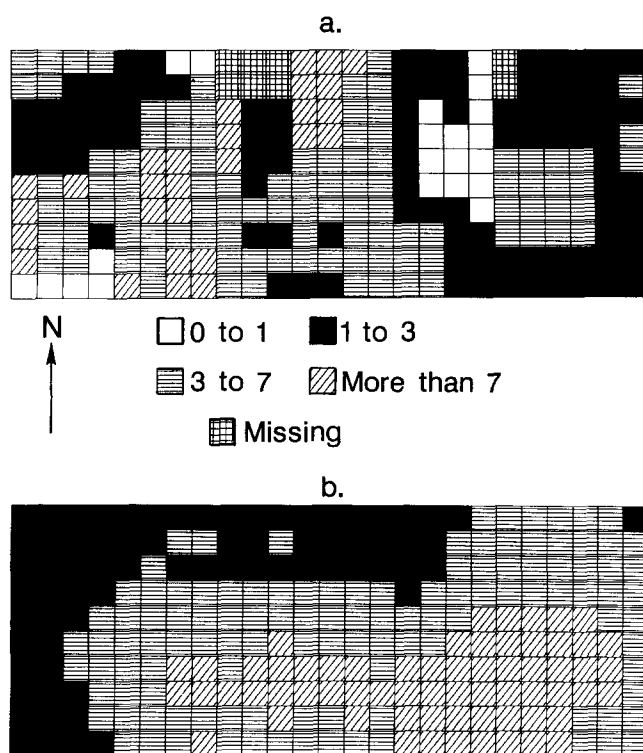


Fig. 10. Kriged distributions of breakthrough (first arrival) time (days) for water (a) and Br^- tracer (b) in compacted, spatially variable clay liner.

mosaics of respective distributions. Numerical values for both fall within a similar range. However, because of differences in frequency and continuity limitations, kriged values for tracer breakthrough are essentially extrapolations beyond effective range of tracer variogram. They differ from water breakthrough at the same location and show no particular pattern, while those for water appear to be somewhat sensitive to small changes in hydraulic gradient that result from local differences in clay thickness.

Water level was maintained constant over the clay following ponding. Preliminary calculations showed that, with assumed flux (q) through the clay matrix on the order of $1 \times 10^{-9} \text{ m s}^{-1}$, water could take as long as 10 years to pass through the experimental 30-cm-thick clay liner. Since considerably faster flow rates and breakthrough times were observed experimentally at several locations, it was concluded that short-circuiting flow was taking place through a few relatively larger continuous pores in the otherwise slowly permeable clay matrix. Such continuous pores would be expected to be more sensitive to a hydraulic gradient imposed by ponded water, as the results in Fig. 10b show. In contrast, Br^- tracer moved only through that portion of the profile that was directly influenced by a spiked ring. The head in each ring was controlled separately. Tracer would have to diffuse into the clay matrix if the infiltration ring was not situated directly over or close to a macropore. Consequently, tracer flow would be far less sensitive to overall hydraulic gradient in ponded water and more sensitive to local conditions associated with each ring.

Water breakthrough times on the average appear to be longer than those for tracer, possibly because of initial radial diffusion of water from macropores into the adjacent, unsaturated clay matrix. Actual tracer breakthrough may well be faster still, since Br^- breakthrough distribution was determined in wet soil. Under these conditions tracer flow could lag behind due to displacement of tracerless water ahead of the infiltrating solution (Ghuman et al., 1975).

Effective porosity

In Table 1, laboratory values of hydraulic conductivity measured on selected 9-cm diameter cores are given along with average flux-density values based on inflow and outflow. These cores were taken within each infiltration ring. Laboratory hydraulic conductivity was determined using a flexible wall permeameter, a gradient of about 20, and an ASTM D18.04.8402 procedure. Results illustrate the extent of discrepancies possible between field and laboratory determinations.

Based on laboratory values (Table 1), breakthrough times for a 30-cm-thick clay layer should be several years. Even if larger field inflow or outflow rates such as those in columns 3 and 4 of Table 1 were used in calculations, breakthrough times of 336 and 552 hours, respectively, would be expected. Consequently, considerably faster observed breakthrough times for water and tracer suggest relatively low effective porosity. Table 2 gives computed values of effective flux density (q_e), observed breakthrough times, and relative amounts

TABLE 1

Laboratory values of hydraulic conductivity¹ compared with average² field values of ring inflow and drain outflow

Site	Lab	Field	
		Ring inflow (10^{-9} ms^{-1})	Drain outflow (10^{-9} ms^{-1})
A1	1.1	40.1	164.4
A2	2.2	59.5	99.1
A3	5.9	235.2	105.7
A4	1.7	215.5	140.9
A5	2.6	155.0	149.2
A6	2.0	85.7	41.8
A7	0.4	4.0	98.4
C2	1.7	4.7	0.1
C5	1.8	6.8	0.6
C7	2.7	97.8	109.4
E3	1.5	7.0	0.0
F1*	1.0	0.1	2.2
F3	0.8	0.4	0.6
G2	2.6	0.7	0.6
G5*	4.2	43.4	40.8
G6	2.2	95.9	33.7
H5*	1.2	20.0	30.0
I2	0.5	0.3	0.3
J1	1.1	10.8	0.8
K6	1.2	43.4	39.9
N1	0.9	19.5	11.8
N7	1.2	155.4	62.0
S7	0.8	0.3	4.5
T2	1.5	1.1	0.4
V5	2.4	1.7	18.3
W1	0.8	9.3	12.0
Average	1.8 ± 1.2	50.5 ± 69.2	44.9 ± 53.2

¹ Laboratory values obtained using flexible membrane hydraulic conductivity apparatus, ASTM D18.04.8402.

² Field values are for the "430" data set in which total inflow or outflow per unit area for the period of 6/11/85 to 4/30/86 was divided by total elapsed time.

of tracer recovered in leachate from selected drains, and Fig. 11 shows calculated distribution of effective porosity (P_e). Results suggest that over 44% of the site, flow took place through less than 1% of the area. But, at a few locations, flow may have occurred through 10% or more of the local cross-sectional area despite assumed uniform compaction and water content of the clay liner material. Two such locations, F1 (where flow occurred through less than 1% of the area) and G5 (where flow occurred through 5–10% of the area), will now be discussed in detail and compared.

TABLE 2

Breakthrough times (T_b) for Br^- tracer and water, and cumulative tracer concentration (C/C_0). Recovered and computed effective flux density (q_e) values for selected sites based on tracer breakthrough times and average 30 cm thickness of clay

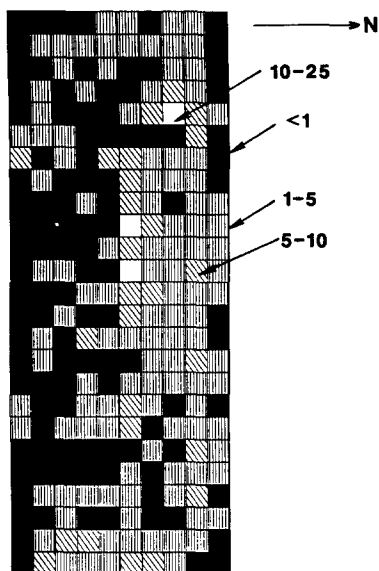
Site	T_b			q_e (10^{-9} m s^{-1})
	Tracer (hr)	Water (hr)	C/C_0 (%)	
AA7	26	45	5	3.205
A3	30	22	43	2.778
D7	29	142	24	2.874
F1*	25	191	2	3.333
G5*	47	142	84	1.773
J0	170	46	2	490
L3	> 265	170	2	> 314
M7	53	71	29	1.572
O1	48	311	< 1	1.736
O9	48	46	10	1.736
Q5	7	144	4	11.904
S1	54	316	2	1.543
T5	161	195	1	517
V8	167	144	3	499
X3	25	144	6	3.333

Macropore flow

To illustrate graphically the flow through soil containing macropores, we have chosen two sites that exhibit contrasting behavior — F1 and G5. Figure 12 shows respective distributions of ring inflow (R), drain outflow (D), and bulk density east (D_E) and west (D_W) of the flow-monitoring site. For the site F1 (Fig. 12a) there appears to be a general agreement between lab and field values, largely because both inflow and outflow distributions are very low. This agreement between lab and field values could be related to rather stable bulk density surrounding the site and to a relatively small effective cross-sectional area involved in flow. The upper curves in Fig. 12a, which give changes in bulk density with time adjacent to the ring and drain location, show that except immediately following ponding, bulk density both east and west of the site remained essentially the same for a whole year. Despite the high uniformity of clay material, a breakthrough time of 25 hours for Br^- at the F1 drain was recorded, although only 2% of the tracer was subsequently recovered (Table 2). These values translate to 0.1% effective porosity with most Br^- expected to be retained in surrounding soil.

In contrast, at the site G5 (Fig. 12b), considerable inflow and outflow existed and density increased quickly at ponding and then more slowly during the remainder of the study. Such increases, alluded to before when discussing site H5 (Fig. 7) and also observed at other sites, are probably indicative of surface

EFFECTIVE POROSITY %
DRAIN250 SUMMATION 4/30/86



EFFECTIVE POROSITY %
DRAIN250 SUMMATION 4/30/86

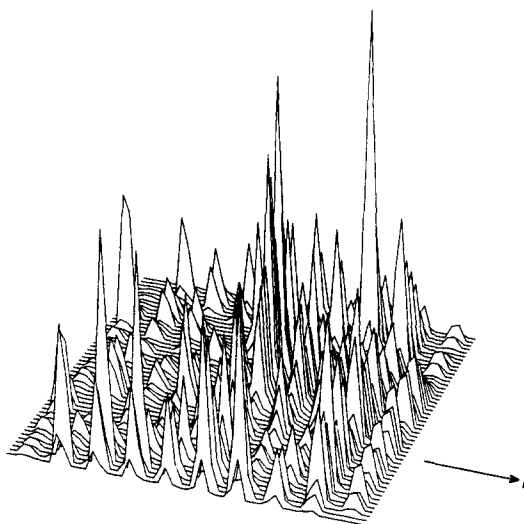


Fig. 11. Distribution of effective porosity (P_e) in a compacted and ponded, spatially variable clay liner given as the percent of cross-sectional area (A), based on first arrival times of ponded water.

wetting and inflow into macropores at ponding, with subsequent movement of water, either as a wetting front or by diffusion from macropores into compacted clay matrix.

Fluctuations of flow in Figs. 7 and 12b may be due to causes described earlier. However, while decline in flow rate after December 1985 was rather abrupt at the site H5, it was much slower and more gradual at the site G5, possibly indicating conflicting effects of different causes. Infiltration was monitored until May 1986 and outflow was measured through August. Some sites had increased flow rates during that summer similar to those shown in Figs. 7 and 12b, suggesting possible sensitivity to changes in viscosity. Such sensitivity would only be apparent for flows that were relatively more rapid and that took place in the macropores.

Tracer distributions

Figure 13 shows relative cumulative concentration of tracer in drains under and around the infiltration rings F1 and G5, to which tracer was originally applied. Although the first breakthrough occurred in 25 hours from the drain

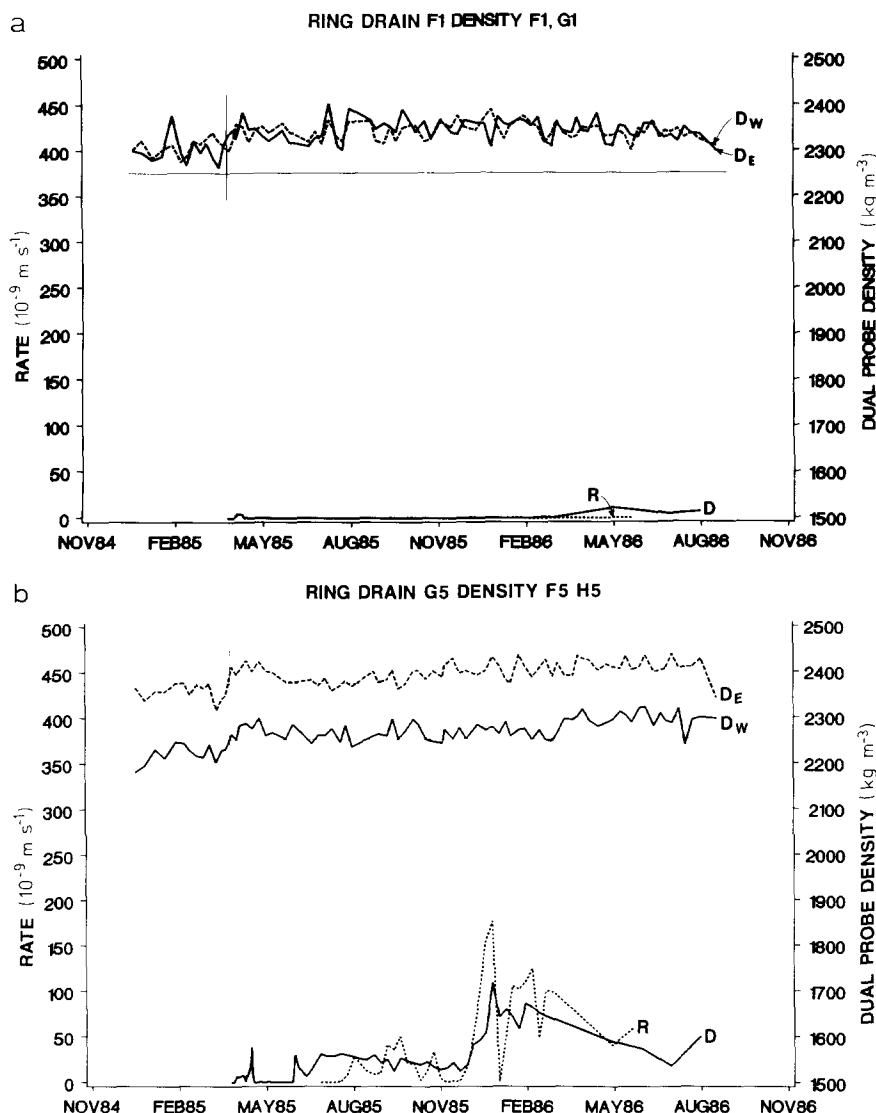


Fig. 12. Distribution in time of ring inflow (R), drain outflow (D), and bulk density to the east (D_E) and west (D_W) of the primary ring and drain locations for the slow-flowing site F1 (a) and fast-flowing site G5 (b).

F1 (directly under the ring to which tracer was applied), the largest amount of tracer (approximately 1% of that applied) came from drain F0 (Fig. 3a).

Effective porosity calculations generally assume vertical flow. Results in Figs. 13a and 13b suggest that this may not always be the case. For example, although 84% of applied tracer was recovered from the drain G5 (directly under

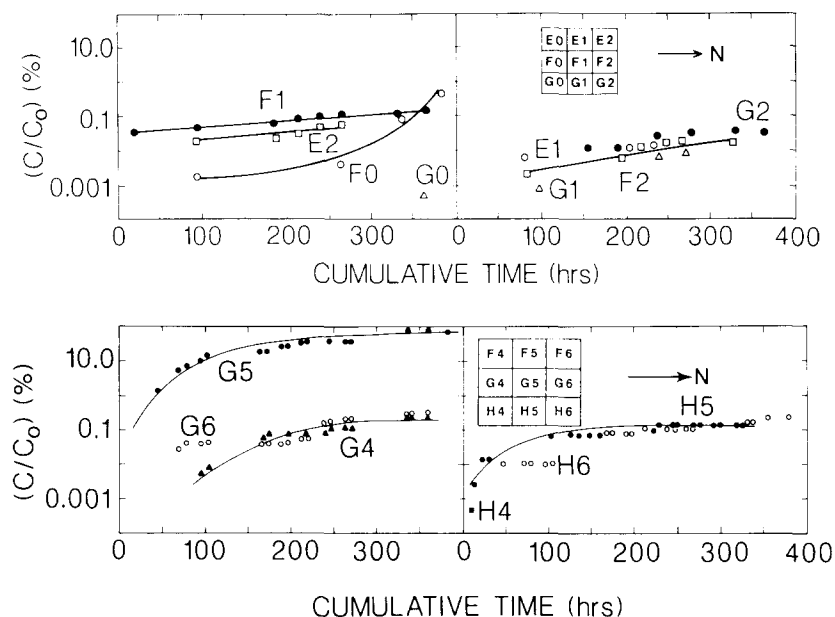


Fig. 13. Relative concentration of Br^- as leachate from site F1 and surrounding drains (a) and site G5 and surrounding drains (b).

the ring G5 to which tracer has been applied), the first arrival of Br^- tracer occurred at drain H5. Small amounts of applied tracer (approximately 0.5%) came from drains G4, G6, and H6.

At the site H5 (Fig. 13b), a relatively rapid (22 hours) first breakthrough of Br^- , which had been applied to a G5 ring, was observed with a computed effective flux density (q_e) greater than or equal to $10,000 \times 10^{-9} \text{ m s}^{-1}$ (assuming a diagonal tracer flux from ring G5 to drain H5). Since observed water outflow flux (q) at H5 at that time was no more than $10 \times 10^{-9} \text{ m s}^{-1}$, effective porosity (P_e) of the area through which the tracer must have passed could be as little as 0.1% of the local cross-sectional area. Even at peak water outflow rate of about $125 \times 10^{-9} \text{ m s}^{-1}$ (Fig. 7) the effective porosity (P_e) values would have been no more than about 1%.

Such calculations may explain in part the absence of any major changes in bulk density adjacent to the sites F1 and G5 (Fig. 12). In terms of environmental safety, the flow rate of concern would be the $10,000 \times 10^{-9} \text{ m s}^{-1}$ breakthrough time for tracer rather than the very slow (approximately $1 \times 10^{-9} \text{ m s}^{-1}$) matrix flow component. However, in real-life situations, when we may wish to evaluate potential impact on groundwater, such high flow rates may need to be considered in terms of cross-sectional areas (effective porosity) that contribute to flow ($\leq 1\%$) and the observed concentration of contaminant in recharge.

Breakthrough history at sites F1 and G5 and surrounding drains, as well as order of magnitude differences between lab and field values in Table 1, suggest

that a seemingly uniform clay liner is a highly variable one with an effective porosity that ranges from as little as 0.1% to more than 5%. Results suggest that, if potential impacts on groundwater from these sites are considered, breakthrough times, delivered concentrations, and contaminant toxicity should all be carefully evaluated.

Subsequent coring with a Veihmeier tube of the tracer application area and surrounding sites on the 0.3-m grid and qualitative tests (Goldman and Byles, 1959) for Br^- corroborated preliminary observations. On sites such as F1, where little tracer was lost as leachate, strong evidence of tracer shows in corings as a tight, well-defined "plume" surrounding the infiltration ring to which tracer has been added (Fig. 14a). However, for sites such as G5, where much tracer was lost as leachate, the Br^- distribution plume was quite extensive but rather diffuse throughout the area of nine drains (Fig. 14b). Highly mobile tracers (or highly mobile contaminants) may be more difficult to detect close to the source of application, even though their impact could be greater and felt sooner further away. Additional corroboration of these

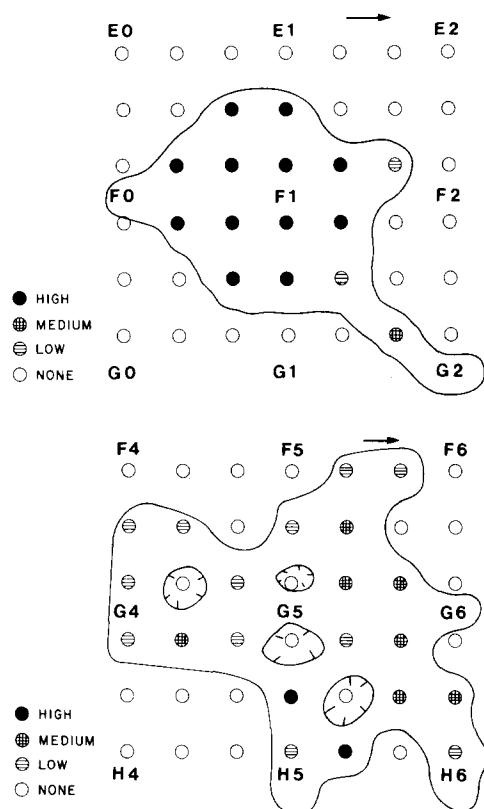


Fig. 14. Relative distribution of Br^- tracer in soil around the sites F1 (a) and G5 (b) to which tracer has been applied.

findings may be found in data on the quality of chemical leachate from the compacted clay (Rogowski, 1986b).

Potential impacts on groundwater

Extrapolating developed concepts to field situations, it may be said that the impact of a field site on groundwater quality may be dictated by its potential to raise contaminant concentration above some predetermined threshold level. The impact may also need to be evaluated from a standpoint of how quickly can a given field site "deliver" contaminant to groundwater. Consequently, sites that exhibit a high probability of outflow rate that exceeds a predetermined threshold value of outflow can be regarded as having a potential for greater impact. For example, impact of a site such as F1 on overall water quality may be minimal. But closer examination of inflows and outflows from sites such as G5 and H5 may be called for. A site such as G5 could have a considerably larger impact on groundwater quality than a site F1 because of rapid potential delivery as well as higher delivered concentration.

SUMMARY AND CONCLUSIONS

The study of a compacted and ponded clay liner provided sufficiently extreme conditions to shed light on the process of preferential pathway flow. Relatively few macropores survived heavy compaction, thus prevailing clay matrix flux density values of approximately $1 \times 10^{-9} \text{ ms}^{-1}$ were sufficiently different from locations with fluxes one or two orders of magnitude higher. At these locations water and tracer Br^- breakthrough histories established probable magnitudes of effective porosity and effective flux density associated with preferential pathway flow. Although breakthrough times on the order of 7–10 years were expected, considerably faster actual breakthrough times were observed (some as fast as one day), suggesting very small effective porosity (0.1 to 5% of local available pore space). It is assumed that fast breakthrough time values indicated location of preferential flow pathways. These results were corroborated by small changes in bulk density, suggesting that, despite relatively high flux, little flow into the clay matrix took place.

Three scales of observation were used. Individual values of density, inflow, and outflow were measured at 250 grid points through the duration of the study. These results were compared and contrasted with the spatially averaged distributions in time and time-averaged distributions at a point. Space-averaged distributions of density showed that overall density changed about 50 kg m^{-3} during the study period, with about half of the change occurring following ponding and the other half during the first ten months of the study. Because some outflows and inflows were very small, averaging over time produced more stable values that were less sensitive to observational error.

While conclusions of this study are not directly transferable to other sites, the general concepts are. Because of readily definable boundaries and detailed

knowledge of input and output on a fine-enough grid, a new understanding of preferential flow was achieved that may be transferable to other locations. It appears that flows at a point may be — and in fact need to be — averaged over a suitable interval of time whenever flow rates are low or concentrations small. This could be particularly important for pollutant flows under unsaturated conditions. It also appears that spatial averages of bulk density changes may provide a good measure of regional water content changes with time. In contrast, little conclusive information can be derived from individual point values. Finally, as an additional benefit of this study, it appears that compaction of the clay and the very low permeability of the clay matrix highlight the behavior of preferential-flow paths, which act as primary conduits of flow with some interesting side effects. For example, when the population of flow paths is low ($< 1\%$), matrix contribution to leachate quality appears to increase and higher concentrations of tracer are found close to the point of origin. On the other hand, in areas of relatively high effective porosity (approximately 5%), where flow path population is higher, little contribution of matrix to leachate quality is observed, and the concentration of tracer is more spread out and diffuse about the application site. Thus the nature of flow path populations may have an important impact, not only on the rate of flow, but also on flow quality.

ACKNOWLEDGMENTS

This study was supported in part by the Land Pollution Control Division, Hazardous Waste Engineering Research Laboratory, United States Environmental Protection Agency, Cincinnati, Ohio, through Interagency Agreement No. DW129-303-03-01-0 with the Northeast Watershed Research Center, Agricultural Research Service, United States Department of Agriculture, University Park, Pennsylvania; Dr. Walter E. Grube, Jr. is the United States Environmental Protection Agency Project Officer.

This article has not been subjected to Environmental Protection Agency review. Therefore, the contents do not necessarily reflect the view of the Agency and no official endorsement should be inferred.

REFERENCES

- Cressie, N.A.C., 1987. Exact interpolation. *Geostatistics*, VI(4): 11–13.
- Daniel, D.E., 1984. Predicting hydraulic conductivity of clay liners. *J. Geotechn. Eng.*, 110(2): 285–300.
- Ghuman, B.S., Verma, S.M. and Drihar, S.S. 1975. Effect of application rate, initial soil wetness, and redistribution time on salt displacement by water. *Soil Sci. Soc. Am. Proc.*, 39: 7–10.
- Goldman, E. and Byles, D., 1959. Suggested revision of phenol red method for bromide. *J. Am. Water Works Assoc.*, 51: 1051–1053.
- Journel, A.G. and Huijbregts, C.J., 1978. *Mining Geostatistics*. Academic Press, New York, NY, 600 pp.
- Kirkham, D. and Powers, W.L., 1972. *Advanced Soil Physics*. Wiley Interscience, New York, NY, 534 pp.

- Nielsen, D.R., van Genuchten, M.T. and Biggar, J.W., 1986. Water flow and solute transport processes in unsaturated zone. *Water Resour. Res.*, 22(9): 895-1085.
- Philip, J.R., 1987. The quasilinear analysis, the scattering analog and other aspects of infiltration and seepage. In: Yu-Si Fok (Editor), *Proceedings, International Conference on Infiltration, Development and Application*, Univ. of Hawaii at Manoa, Honolulu, Hawaii, pp. 1-27.
- Rogowski, A.S., 1985. Effectiveness of a compacted clay liner in preventing ground water contamination. In: *Proceedings, 5th National Symposium on Aquifer Restoration and Ground Water Monitoring*, National Water Well Association, Worthington, OH, pp. 412-429.
- Rogowski, A.S., 1986a. Hydraulic conductivity of compacted clay soils. In: *Proceedings, 12th Annual Research Symposium*, U.S. Environ. Prot. Agency, EPA-600/9-86-022, Cincinnati, OH, pp. 29-39.
- Rogowski, A.S., 1986b. Degree of saturation, hydraulic conductivity, and leachate quality in a compacted clay liner. In: R.M. Khanbilvardi and J. Fillos (Editors), *Ground Water Hydrology, Contamination, and Remediation*. Scientific Publications Co., Washington, D.C., pp. 339-353.
- Rogowski, A.S. and Richie, E.B., 1984. Relationship of laboratory and field determined hydraulic conductivity in compacted clay soils. In: M.D. LaGrega and D.A. Long (Editors), *Proceedings, 16th Mid-Atlantic Industrial Waste Conference*. Technomic Publ. Co., Inc., Lancaster, PA, pp. 520-533.
- Rogowski, A.S. and Simmons, D.E., 1988. Geostatistical estimates of field hydraulic conductivity in compacted clay. *Math. Geol.*, 20(4): 423-446.
- Rogowski, A.S., Weinrich, B.E. and Simmons, D.E., 1985. Permeability assessment in a compacted clay liner. In: *Proceedings, 8th Annual Madison Waste Conference*, Univ. of Wisconsin, Madison, WI., pp. 315-336.